



Design Of Hyperparameter Tuned Deep Learning Driven Object Detection And Classification Model For Video Surveillance Systems

V. Saikrishnan¹, Dr. M. Karthikeyan²

1-Department of Computer and Information science, Faculty of Science, Annamalai University, Tamil Nadu, INDIA

2-Department of Computer and Information science, Faculty of Science, Annamalai University, Tamil Nadu, INDIA

Abstract—Presently, surveillance videos becomes widespread due to their applicability in different real time scenarios. Investigation of surveillance videos is a tedious process in the domains of computer vision and image processing. Object detection and tracking pose challenging issues in the field of computer vision. The recent developments of machine learning (ML) as well as deep learning (DL) models find useful to design effective object detection approaches. This article designs a Hyperparameter Tuned Deep Learning Driven Object detection and Classification Model for Video Surveillance Systems (HTDLLOC-VSS). The major goal of the HTDLLOC-VSS model is to identify and classify the presence of objects present in the surveillance videos. The HTDLLOC-VSS model primarily applies YOLO-v5 object detector to effectually detect the target objects. Besides, Nadam optimizer is applied to fine tune the hyperparameters of the YOLO-v5 model. In addition, binary particle swarm optimization (BPSO) with multiclass support vector machine (MSVM) model is employed for object classification. The utilization of Nadam and BPSO algorithm assists in the accomplishment of enhanced object detection performance. A wide range of experiments was carried out on benchmark datasets and the results are assessed under several aspects. The comparison study highlighted the enhanced outcomes of the HTDLLOC-VSS model over the other approaches.

Keywords— Object detection, Object classification, Video surveillance, Deep learning, Parameter tuning, YOLO-v5.

I. INTRODUCTION

During the last couple of years, object recognition has witnessed considerable development because of the current development in deep learning-based algorithms. Several studies have investigated object recognition with the consideration of video as image to identify objects in video [1]. But people don't consider every frame as an autonomous image in the procedure of identifying objects in the video, instead trace a most important movement regarding an earlier frame. Consequently, video recognition technologies like intelligent robotics, video surveillance, and automotive driving are an integration of object tracking and detection techniques [2]. In recent times, approaches like single shot detector (SSD), you only look once (YOLO), and region-based convolutional network (R-CNN) have occurred that shows outstanding results in the area of real time object recognition [3]. But higher performing hardware is needed for using them in the video surveillance field.

Object recognition is extensively applied in intelligent monitoring, military object recognition, UAV navigation, unmanned vehicles, and smart transportation [4]. But as a result of the various object detection methods, the existing method fails to recognize the object. Changing light and Complex background rises the complication of object recognition, specifically for objects in stimulating conditions [5, 6]. The tracking technique operates by recognizing an object when it initially appeared in a frame and predicting its trajectory [7]. This detection-based method evaluates the object location in each frame autonomously. It needs an offline training method and couldn't be applied to unidentified objects.

Various detection and tracking methodologies were introduced recently. But the challenging problem encounters during that process means that the fields require considerable research. The problem that complicates detection and tracking includes camera jitter, rapid illumination changes, dynamic backgrounds, shadow detection, moving cameras, etc [8, 9]. Such challenges could not be solved through the simplest method because of the complexities, impreciseness, and improbable factors existing in the intermediate phase. To solve this, deep learning and computation intelligence (CI) methods were introduced [10].

Mou et al. [11] present for training a domain-adoptive scene-specific pedestrian detector in unsupervised method. The generic detector has been relocated for distinct target domain in one labeled source domain data set without human-annotated target sample. In detail, it is primarily expanded the generic detector to dual-boundary classification and gathered hard samples as unlabelled target samples based on the recognition confidence. Next, presented a cycle semantic transfer method for aligning the class-level and instance-level distributions among the target and source domains and labeling the hard sample automatically. Elhoseny [12] presented a MODT method. The presented technique employs an optimum Kalman filtering method for tracking the moving object in video frame. The video clip was transformed according to the amount of frames into morphological operation through the region growing method.

The researchers in [13] presented an effecting technique for movement tracking and object detection. Here, we presented strong video object tracking and detection method. The fuzzy morphological filter was performed to remove the noise existing in the foreground segmented frame. Jha et al. [14] presented a method named N-YOLO that is rather than resizing image step in YOLO, it splits into fixed size image utilized in YOLO and merges detection outcomes of sub-images with inference outcomes at distinct times with relation-based tracking approach the sum of calculation for object tracking and detection is considerably minimized. In [15], a Background Modelling method is presented by a Biased Illumination Field Fuzzy C-means approach for detecting the moving object precisely. Now, the non-stationary pixel is separated from stationary pixel by using Background Subtraction. Next, the Biased Illumination Field Fuzzy C-means technique has been achieved to enhance the segmentation accuracy by clustering in varying and noise illumination conditions.

This article designs a Hyperparameter Tuned Deep Learning Driven Object detection and Classification Model for Video Surveillance Systems (HTDLODC-VSS). The major goal of the HTDLODC-VSS model is to identify and classify the presence of objects present in the surveillance videos. The HTDLODC-VSS model primarily applies YOLO-v5 object detector to effectually detect the target objects. Besides, Nadam optimizer is applied to fine tune the hyperparameters of the YOLO-v5 model. In addition, binary particle swarm optimization (BPSO) with multiclass support vector machine (MSVM) model is employed for object classification. The utilization of Nadam and BPSO algorithm assists in the accomplishment of enhanced object detection performance. A wide range of experiments was carried out on benchmark datasets and the results are assessed in several aspects.

II. THE PROPOSED MODEL

In this study, a new HTDLODC-VSS technique has been developed for the detection and classification of objects present in the surveillance videos. The HTDLODC-VSS technique encompasses YOLO-v5 object detector, Nadam optimizer based hyperparameter tuning, MSVM based classification, and BPSO based parameter tuning.

$$\min(\omega, \xi) = \frac{1}{2}\omega^2 + \beta \sum_{i=1}^n \xi_i$$

A. Object Detection Module

The HTDLODC-VSS model primarily applies YOLO-v5 object detector to effectually detect the target objects. Object detection is most important problem from the domain of computer vision (CV) [16]. It allows the computer for discovering and locating target of interest in an image automatically like flaws from the fabric. DL based object detection techniques are obtained major successes in recent times. But, the above techniques are effort to meet the real time requirement of fabric defect recognition model as it is high computational overhead. For balancing precision and speed, a lightweight object detection network is called YOLOv5, is utilized during this case. The typical YOLOv5 has enhanced dependent upon the features of fabric defect such that it could be executed to fabric defect recognition method. The infrastructure of typical YOLOv5 mostly comprises Backbone, PANet, and Output. The backbone has been utilized for performing feature engineering in input images. The PANet has attained visual feature robust for scale changing because of utilized pyramid infrastructure. The places are output, and the ROI is classification concurrently.

At this stage, Nadam optimizer is applied to fine tune the hyperparameters of the YOLO-v5 model. Nadam is otherwise known as Nesterov Adam optimizer. Much like Adam is basically RMSprop with momentum, Nadam is Adam RMSprop with Nesterov momentum [17].

$$\hat{g}_t \leftarrow \frac{g_t}{1 - \prod_{i=1}^t \beta_{1i}} \quad (1)$$

$$m_t = \beta_1 m_{t-1} + (1 - \beta_1) g_t \quad (2)$$

$$\hat{m}_t = \frac{m_t}{1 - \prod_{i=1}^{t+1} \beta_{1i}} \quad (3)$$

$$v_t = \beta_2 v_{t-1} + (1 - \beta_2) g_t^2 \quad (4)$$

$$\hat{v}_t = \frac{v_t}{1 - \beta_2^t} \quad (5)$$

The vector \bar{m} comprises the gradient update for the existing timesteps \hat{g}_t along with the momentum vector update for the following timestep $\beta t + 1 \hat{m}_t$.

$$\hat{m}_{t-1} \leftarrow (1 - \beta_1) \cdot \hat{g}_t + \beta_{t+1} \cdot \hat{m}_t \quad (6)$$

Next, update variable of Nadam is given by:

$$\theta_t = \theta_{t-1} - \frac{\alpha}{\sqrt{\hat{v}_t} + \varepsilon} \bar{m}_{t-1} \quad (7)$$

The default value of Nadam is $\alpha = 0.002$, $\beta_1 = 0.9$, $\beta_2 = 0.999$, and $\varepsilon = 10^{-8}$

B. Object Classification Module

During object classification process, the MSVM model is applied to allocate class labels. The MSVM classification was depending on Vapnik–Chervonenkis (VC) dimension of the statistical learning scheme. The main goal is to map the pre-processing, non-linear microarray gene expression data to a linear dimension manifold θ with the use of alteration $\phi: R^N \rightarrow \theta$, after accomplishing an optimal hyperplane: $\Psi: \psi(x) = (\omega \cdot \phi(x) + b)$ solve the succeeding augmented convex issue (the soft margin issue) [18]:

Subject to

$$y_i(\omega \cdot \phi(x) + b) \geq 1 - \xi_i, \text{ for all } 1 \leq i \leq n, \quad (8)$$

Whereas ω denotes the coefficient vectors of hyperplane from the manifold, b shows the threshold value of hyperplane, ξ_i denotes the slack problem offered to classification error, and β denotes the penalty factor to error. The variable β controls the penalty of misclassified and the value was generally determined by cross-validation. The larger value of β leads to a smaller margin that reduces classification error, however low values of β generate a wider margin result from different misclassified. Fig. 1 depicts the hyperplane of SVM.

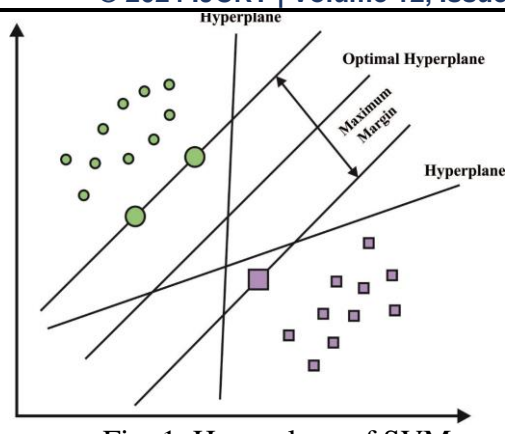


Fig. 1. Hyperplane of SVM

The feature space θ was very dimension; henceforth, the direct estimation results in “dimension disaster.” Then, $\omega = \sum_{i=1}^n \delta_i y_i \phi(x_i)$, each process of MSVM in the feature space θ is dot product. Next, kernel function that is, $(x_i, x_{i'}) = \phi(x_i) \cdot \phi(x_{i'})$, are efficient at managing dot product, it is proposed to SVM. Thus, the selection of kernel and the coefficient was indispensable in the computation accuracy and performance of MSVM classifier methods.

The kernel function is exploited as a constant predictor:

The linear kernel is determined by.

$$G(x_i, x_{i'}) = x_i \cdot x_{i'}. \quad (9)$$

Then, the polynomial kernel is given in the following:

$$G(x_i, x_{i'}) = (\eta * (x_i \cdot x_{i'}) + \delta)^d, \quad (10)$$

When $\eta > 0, \delta \in R$, and $d \in Z^+$.

Next, the Gaussian kernel is equated by.

$$G(x_i, x_{i'}) = \exp\left(\frac{x_i - x_{i'}^2}{2\sigma^2}\right), \quad (11)$$

When $\sigma > 0$.

The MSVM kernel function is almost taken into the following: local and global kernel functions. Instance extensively distinct has a major effect on the global kernel value however, sampled near one another considerably control the local kernel value. The polynomial and linear kernels are optimal samples of global kernels, however, the Gaussian and Gaussian radial basis function (RBF) are local kernels.

C. Parameter Tuning Model

Finally, the BPSO algorithm is utilized to tune the parameters involved in the MSVM model. Binary particle swarm optimization is a heuristic search approach since its good performance in global search ability and searches velocity [19]. In general, there are N particles with index i for all the particles, that is., $i = 1, 2, \dots, N$. Also $X_i^m = (x_{i1}^m, x_{i2}^m, \dots, x_{ij}^m, \dots, x_{iK}^m)$ denotes the location vector of particle i in iteration m , whereby the dimension of the particle is K , that need to be the amount of features (K) in FS problem and $x_{ij}^m \in \{0,1\}$. Hence, $(X_1^m, X_2^m, \dots, X_N^m)$ denotes the swarm of the particle in iteration m , and next P_i^m characterize the personal optimal location for particle i in iteration m , whereby $P_i^m = (p_{i1}^m, p_{i2}^m, \dots, p_{ij}^m, \dots, p_{iK}^m)$ and $p_{ij}^m \in \{0,1\}$. Furthermore, there is G^m that represents the global optimal location in iteration m , in which $G^m = (g_1^m, g_2^m, \dots, g_j^m, \dots, g_K^m)$ and $g_j^m \in \{0,1\}$. In all the iterations m , the velocity vector of particle i , V_i^{m+1} is upgraded by:

$$V_i^{m+1} = wV_i^m + c_1r_1(P_i^m - X_i^m) + c_2r_2(G^m - X_i^m), \quad (12)$$

Whereas $V_i^m = (v_{i1}^m, v_{i2}^m, \dots, v_{ij}^m, \dots, v_{iK}^m)$ denotes the preceding velocity vector in iteration m , w represent the inertia weight coefficient, c_1 denotes the weight factor for personal optimal location, c_2 indicates the weight factor for global optimal location, as well, r_1 and r_2 denotes arbitrary value distributed uniformly within $[0,1]$.

There are generally maximum and minimum limits for velocity vector, V_{\max} and V_{\min} , that is determined to limit the velocity V_i^{m+1} , if V_i^{m+1} in (12) is higher than V_{\max} , then $V_i^{m+1} \rightarrow V_{\max}$, or if V_i^{m+1} is lesser than V_{\min} , then $V_i^{m+1} \rightarrow V_{\min}$. Also, the inertia weight w upgraded as follows:

$$w^m = w_{\max} - (w_{\max} - w_{\min}) * (m - 1)/M, \quad (13)$$

Here w_{\max} and w_{\min} denotes maximal and minimal limits for the inertia weight, M indicates the maximal amount of iterations. The location of i th particle upgrade is as follows:

$$X_i^{m+1} = X_i^m + V_i^{m+1}, (14)$$

Whereas in the binary form of PSO, the velocity vector needs to be converted into a probability vector via a sigmoid function.

$$s_{ij}^{m+1} = (1 + e^{v_{ij}^{m+1}})^{-1}, (15)$$

Now s_{ij}^{m+1} denotes the probability that the x_{ij}^{m+1} is 1. Hence, the location of i th particle upgrade is as follows:

$$x_{ij}^{m+1} = \begin{cases} \text{if } \delta < s_{ij}^{m+1} & j = 1, \dots, K \\ 0, & \text{otherwise} \end{cases} (16)$$

Now δ indicate an arbitrary value distributed uniformly within $[0,1]$.

III. PERFORMANCE VALIDATION

The performance validation of the HTDLLOC-VSS model is tested using the UCSDPed2 dataset [20], which contains two subsets namely pedestrian-1 and pedestrian-2 datasets. Table 1 depicts the dataset description. Fig. 2 shows the sample test image with respective ground truth images. Fig. 3 visualizes the sample outcomes of the HTDLLOC-VSS model. The figure indicated that the HTDLLOC-VSS model has detected all the objects that exist in the video frame.

TABLE I

DESCRIPTION OF DATASET

Dataset	Testbed	Frames No.	Time (sec)
UCSDped2	Pedestrian-1 Dataset	360	12
	Pedestrian-2 Dataset		



Fig. 2. a) Original Image b) Ground Truth Image



Fig. 3. a) Original Image b) Tracking Image

Fig. 4 highlights the average detection accuracy of the HTDLLOC-VSS model on two sub datasets. The figure indicated that the HTDLLOC-VSS model has reached maximum performance over the other methods on two sub datasets. For instance, with surveillance ped-1 dataset, the HTDLLOC-VSS model has offered higher average accuracy of 98.56% whereas the CIHSA-RTODT, DLADT, Region CNN, and FR-CNN models have obtained lower average accuracy of 98%, 97%, 97%, and 85%. Also, with surveillance ped-2 dataset, the HTDLLOC-VSS method has offered higher average accuracy of 93.72% whereas the CIHSA-RTODT, DLADT, Region CNN, and FR-CNN approaches have gained lesser average accuracy of 91%, 90%, 87%, and 82%.

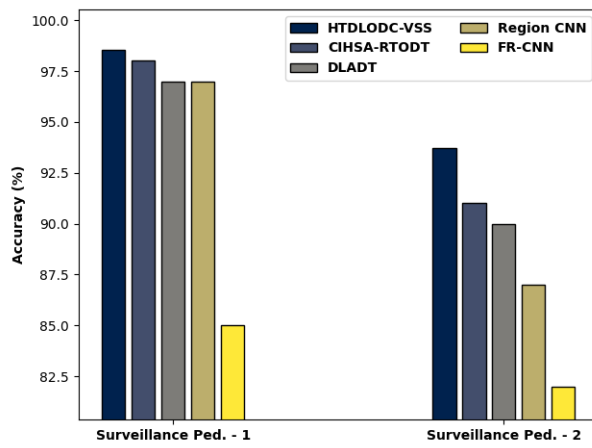


Fig. 4. Average accuracy of HTDLODC-VSS model on two sub datasets

TABLE II

AUC ANALYSIS OF HTDLODC-VSS MODEL ON TWO SUB DATASETS

Models	Surveillance Ped.-1	Surveillance Ped.-2
MPPCA Model	61.01	69.92
SF Model	66.74	55.96
SFMPPCA	67.25	61.33
MDT Model	82.05	82.99
AMDN Model	91.71	91.25
ADVAE Model	95.39	92.47
CIHSA-RTODT	97.12	93.92
HTDLODC-VSS	98.35	95.64

Table 2 and Fig. 5 examine the AUC of the HTDLODC-VSS system on two sub datasets. The figure represented that the HTDLODC-VSS technique has reached maximal performance over the other methods on two sub datasets. For instance, with surveillance ped-1 dataset, the HTDLODC-VSS approach has presented higher AUC of 98.35% whereas the MPPCA, SF, SFMPPCA, MDT, AMDN, ADVAE, and CIHSA-RTODT models have obtained lower AUC of 61.01%, 66.74%, 67.25%, 82.05%, 91.71%, 95.39%, and 97.12%. Likewise, with surveillance ped-2 dataset, the HTDLODC-VSS model has offered higher AUC of 95.64% whereas the MPPCA, SF, SFMPPCA, MDT, AMDN, ADVAE, and CIHSA-RTODT approaches have gained minimum AUC of 69.92%, 55.96%, 61.33%, 82.99%, 91.25%, 92.47%, and 93.92%.

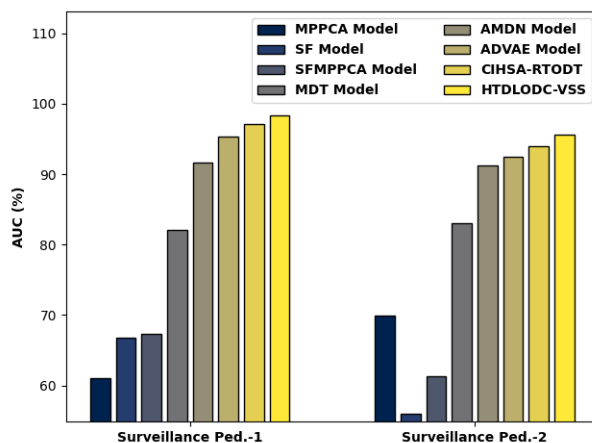


Fig. 5. AUC analysis of HTDLODC-VSS model on two sub datasets

Fig. 6 provides a running time (RT) examination of the HTDLODC-VSS model over the other techniques. The experimental results indicated that the HTDLODC-VSS model has provided lower RT over the other methods. For instance, with surveillance ped-1 dataset, the HTDLODC-VSS model has provided minimal RT of accuracy of 2.14s whereas the MDT, SCLF, AMDN, ADVAE, and CIHSA-RTODT models have accomplished lower RT of 20.61s, 20.11s, 11.73s, 3.94s, and 2.67s respectively. At the same time, with surveillance ped-2 dataset, the HTDLODC-VSS approach has provided minimal RT of accuracy of 2.77s whereas the MDT, SCLF, AMDN, ADVAE, and CIHSA-RTODT techniques have accomplished lower RT of 22.94s, 18.48s, 13.02s, 6.16s, and 3.98s correspondingly.

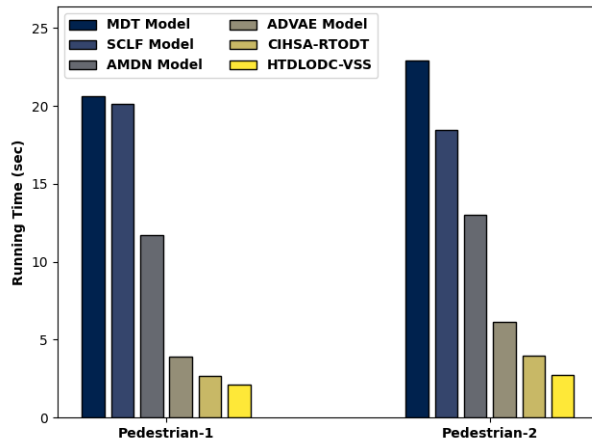


Fig. 6. RT analysis of HTDLODC-VSS model on two sub datasets

Fig. 7 highlights the comparative result examination of the HTDLODC-VSS model with existing models on surveillance Ped.-1 dataset [21-24]. The figure indicated that the HTDLODC-VSS model has accomplished maximum ROC values. The results indicated that the SF model has showcased poor outcomes with lower ROC values. Followed by, the ADVAE and CIHSA-RTODT model have demonstrated slightly enhanced ROC values. In line with, the AMDN model has accomplished reasonable ROC values. However, the HTDLODC-VSS model has reached maximum performance over the other methods.

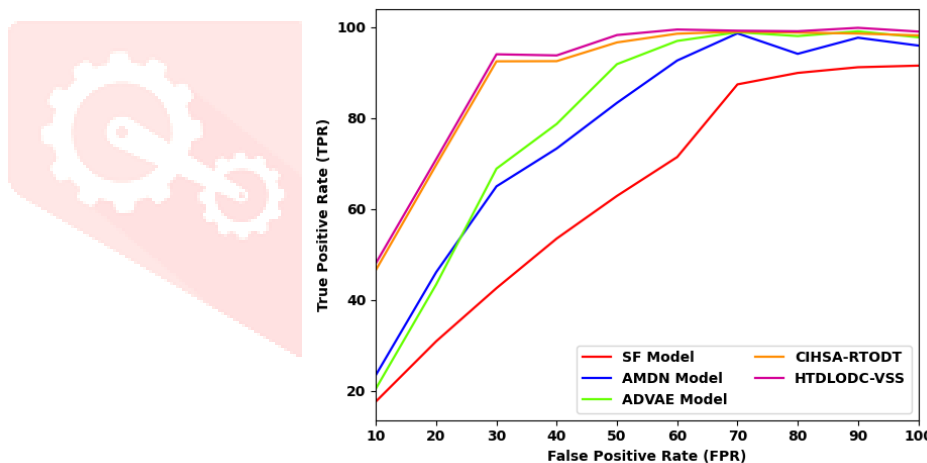


Fig. 7. Comparative analysis of HTDLODC-VSS technique on surveillance Ped.-1 dataset

Fig. 8 reports the comparative result examination of the HTDLODC-VSS approach with existing techniques on surveillance Ped.-2 dataset. The figure exposed that the HTDLODC-VSS model has accomplished maximum ROC values. The results exposed that the SF approach has demonstrated poor outcomes with reduced ROC values. Followed by, the ADVAE and CIHSA-RTODT model have demonstrated slightly improved ROC values. Likewise, the AMDN model has accomplished reasonable ROC values. Finally, the HTDLODC-VSS algorithm has reached maximal performance over the other methods.

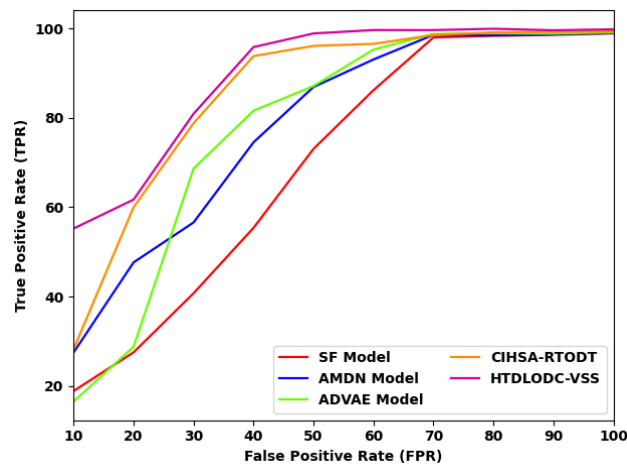


Fig. 8. Comparative analysis of HTDLODC-VSS technique on surveillance Ped.-2 dataset

4. Conclusion

In this study, a new HTDLODC-VSS technique has been developed for the detection and classification of objects present in the surveillance videos. The HTDLODC-VSS technique encompasses YOLO-v5 object detector, Nadam optimizer based hyperparameter tuning, MSVM based classification, and BPSO based parameter tuning. The utilization of Nadam and BPSO algorithm assists in the accomplishment of enhanced object detection performance. A wide range of experiments was carried out on benchmark datasets and the results are assessed under several aspects. The comparison study highlighted the enhanced outcomes of the HTDLODC-VSS model over the other approaches. Therefore, the HTDLODC-VSS model has appeared as a proficient method of accomplishing maximum object detection performance. In future, the detection efficiency can be improved by hybrid DL approaches.

REFERENCES

- [1] Jha, S., Seo, C., Yang, E. and Joshi, G.P., 2021. Real time object detection and tracking system for video surveillance system. *Multimedia Tools and Applications*, 80(3), pp.3981-3996.
- [2] Xu, J., 2021. A deep learning approach to building an intelligent video surveillance system. *Multimedia Tools and Applications*, 80(4), pp.5495-5515.
- [3] Naik, U.P., Rajesh, V. and Kumar, R., 2021, September. Implementation of YOLOv4 Algorithm for Multiple Object Detection in Image and Video Dataset using Deep Learning and Artificial Intelligence for Urban Traffic Video Surveillance Application. In *2021 Fourth International Conference on Electrical, Computer and Communication Technologies (ICECCT)* (pp. 1-6). IEEE.
- [4] Wang, Y., Mao, K., Chen, T., Yin, Y., He, S. and Chen, G., 2021. Accelerating real-time object detection in high-resolution video surveillance. *Concurrency and Computation: Practice and Experience*, p.e6307.
- [5] Gautam, A. and Singh, S., 2021. Deep Learning Based Object Detection Combined with Internet of Things for Remote Surveillance. *Wireless Personal Communications*, 118(4), pp.2121-2140.
- [6] Xu, J., 2021. A deep learning approach to building an intelligent video surveillance system. *Multimedia Tools and Applications*, 80(4), pp.5495-5515.
- [7] Gautam, A. and Singh, S., 2021. Deep Learning Based Object Detection Combined with Internet of Things for Remote Surveillance. *Wireless Personal Communications*, 118(4), pp.2121-2140.
- [8] Sung, C.S. and Park, J.Y., 2021. Design of an intelligent video surveillance system for crime prevention: applying deep learning technology. *Multimedia Tools and Applications*, 80(26), pp.34297-34309.
- [9] Salido, J., Lomas, V., Ruiz-Santaquiteria, J. and Deniz, O., 2021. Automatic handgun detection with deep learning in video surveillance images. *Applied Sciences*, 11(13), p.6085.
- [10] Jiao, L., Zhang, R., Liu, F., Yang, S., Hou, B., Li, L. and Tang, X., 2021. New generation deep learning for video object detection: A survey. *IEEE Transactions on Neural Networks and Learning Systems*.
- [11] Mou, Q., Wei, L., Wang, C., Luo, D., He, S., Zhang, J., Xu, H., Luo, C. and Gao, C., 2021. Unsupervised domain-adaptive scene-specific pedestrian detection for static video surveillance. *Pattern Recognition*, 118, p.108038.
- [12] Elhoseny, M., 2020. Multi-object detection and tracking (MODT) machine learning model for real-time video surveillance systems. *Circuits, Systems, and Signal Processing*, 39(2), pp.611-630.

- [13] Mahalingam, T. and Subramoniam, M., 2020. A robust single and multiple moving object detection, tracking and classification. *Applied Computing and Informatics*.
- [14] Jha, S., Seo, C., Yang, E. and Joshi, G.P., 2021. Real time object detection and tracking system for video surveillance system. *Multimedia Tools and Applications*, 80(3), pp.3981-3996.
- [15] Kalli, S., Suresh, T., Prasanth, A., Muthumanickam, T. and Mohanram, K., 2021. An effective motion object detection using adaptive background modeling mechanism in video surveillance system. *Journal of Intelligent & Fuzzy Systems*, (Preprint), pp.1-13.
- [16] Kuznetsova, A., Maleva, T. and Soloviev, V., 2020, December. Detecting apples in orchards using YOLOv3 and YOLOv5 in general and close-up images. In *International Symposium on Neural Networks* (pp. 233-243). Springer, Cham.
- [17] Xiao, B., Liu, Y. and Xiao, B., 2019. Accurate state-of-charge estimation approach for lithium-ion batteries by gated recurrent unit with ensemble optimizer. *Ieee Access*, 7, pp.54192-54202.
- [18] Thirumala, K., Pal, S., Jain, T. and Umarikar, A.C., 2019. A classification method for multiple power quality disturbances using EWT based adaptive filtering and multiclass SVM. *Neurocomputing*, 334, pp.265-274.
- [19] Akbari, H., Sadiq, M.T., Payan, M., Esmaili, S.S., Baghri, H. and Bagheri, H., 2021. Depression Detection Based on Geometrical Features Extracted from SODP Shape of EEG Signals and Binary PSO. *Traitement du Signal*, 38(1).
- [20] <http://www.svcl.ucsd.edu/projects/anomaly/dataset.html>
- [21] Pustokhina, I.V., Pustokhin, D.A., Vaiyapuri, T., Gupta, D., Kumar, S. and Shankar, K., 2021. An automated deep learning based anomaly detection in pedestrian walkways for vulnerable road users safety. *Safety Science*, 142, p.105356.
- [22] Xu, M., Yu, X., Chen, D., Wu, C. and Jiang, Y., 2019. An efficient anomaly detection system for crowded scenes using variational autoencoders. *Applied Sciences*, 9(16), p.3337.
- [23] Murugan, B.S., Elhoseny, M., Shankar, K. and Uthayakumar, J., 2019. Region-based scalable smart system for anomaly detection in pedestrian walkways. *Computers & Electrical Engineering*, 75, pp.146-160.
- [24] Alotaibi, M.F.; Omri, M.; Abdel-Khalek, S.; Khalil, E.; Mansour, R.F. Computational Intelligence-Based Harmony Search Algorithm for Real-Time Object Detection and Tracking in Video Surveillance Systems. *Mathematics* 2022, 10, 733. <https://doi.org/10.3390/math10050733>